Electronic Supplementary Material (ESI) for Nanoscale.

On a local (de-)trapping model for highly doped Pr^{3+} radioluminescent and persistent luminescent nanoparticles

Gabrielle A. Mandl,[a] David Van der Heggen, [b] Daniel R. Cooper[c], Jonas J. Joos,[b] Jan Seuntjens[c], Philippe F. Smet[b] and John A. Capobianco*[a]

Electronic Supporting Information

Contents

1. Detailed Synthesis of $NaLuF_4$:20% Pr^{3+} Nanoparticles
2. Energy Dispersive Spectroscopy Elemental Mapping of Samples (Figure S1)
3. Inductively coupled plasma mass spectrometry Data (Table S1)
4. Photoluminescence emission spectrum (Figure S2)
5. Powder X-ray diffraction before and after X-ray irradiation (Figure S3)
6. Kinetic profiles of samples 1-4 (Figure S4)
7. Band gap energy extrapolation data (Table S2)
8. Radioluminescence spectrum before and after persistent luminescence (Figure S5)
9. Thermoluminescence data (Figure S6)
10. Powder X-ray Diffraction of undoped $NaLuF_4$ nanoparticles
11. TEM image of undoped $NaLuF_4$ nanoparticles
12. References

1. Detailed synthesis of $NaLuF_4$:20% Pr^{3+} nanoparticles

0.8 mmol $LuCl_3 \bullet x\ H_2O$ and 0.2 mmol $PrCl_3 \bullet xH_2O$ were mixed with 6 mL oleic acid and 15 mL 1-octadecene in a 250 mL 3-neck round bottom flask. The solution was stirred at 500 RPM for the duration of the reaction. First, the solution was heated to 120 °C under vacuum and left to stir for 30 minutes. The solution was then cooled to 90 °C, and the vacuum was removed. Solid sodium oleate and solid ammonium fluoride were then added to the solution and left to stir for 45 minutes under an Argon flow. The vacuum was then re-introduced and the solution was degassed at 120 °C for an additional 30 minutes. The vacuum was then removed and an Argon flow was introduced. The solution was then heated to 320 °C (samples 1 and 2) or 330 °C (3 and undoped) at a temperature ramp of 700 °C/hr and stirred for 2 hours. Sample 4 was heated to 310 °C at a rate of 1000 °C/hr and stirred for 2 hours. All samples were precipitated in 99% ethanol and centrifuged at 4000 RPM for 10 minutes to collect a solid white pellet. The supernatant was discarded and the pellet was dispersed in 5 mL hexanes then re-precipitated by adding 40 mL of 99% ethanol. The suspension was then centrifuged again at 4000 RPM for 10 minutes. This process was repeated 3 times to yield purified oleate-capped $NaLuF_4$: 20% Pr^{3+} and undoped $NaLuF_4$ nanoparticles. Samples were stored as dried powders at room temperature. The different sizes of nanoparticles were obtained by changing the Na:Ln:F ratio and the reaction temperature, as described by Haase *et al.*[1] Increasing the amount of Na and F relative to Ln ions is known to decrease the nanoparticle size and favor the formation of hexagonal phase nanoparticles. Samples 1 and 2 were prepared using a ratio of 2.5 mmol Na^+ : 1 mmol Ln^{3+} : 4 mmol F^-. Sample 3 and the undoped sample was prepared using a ratio of 6 mmol Na^+ : 1 mmol Ln^{3+} : 11 mmol F^-. Sample 4 was prepared using a ratio of 2 mmol Na^+ : 1 mmol Ln^{3+} : 11 mmol F^-.

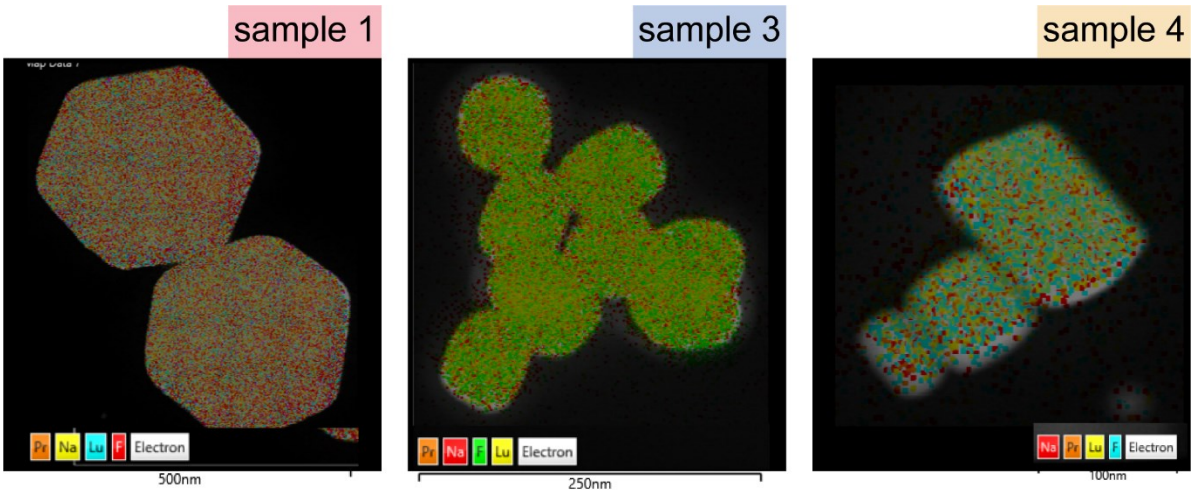

Figure S1. Energy dispersive spectroscopy elemental mapping of samples 1, 3 and 4 demonstrating the uniformity of Na, Lu, F, and Pr ions within the nanocrystals.

2. Energy dispersive spectroscopy elemental mapping of samples

3. Inductively coupled plasma mass spectrometry data

Sample	Pr^{3+} (ppm)	Lu^{3+} (ppm)	% Pr^{3+}	Average % Pr^{3+}
Sample 1A	0.926	4.354	20.88	20.90
Sample 1B	0.689	3.235	20.91	
Sample 2A	0.520	2.325	21.73	21.71
Sample 2B	0.504	2.258	21.68	
Sample 3A	--	--	--	18.90
Sample 3B	0.1559	0.6689	18.90	
Sample 4A	0.349	1.748	19.86	19.94
Sample 4B	0.196	0.973	20.02	
Undoped A	0.00010	1.843	0.0058	0.0039
Undoped B	0.00002	1.026	0.002	

Table S1. Inductively coupled plasma mass spectrometry (ICP-MS) data used to calculate the actual composition of the nanoparticles. ICP-MS was performed in duplicates and values were averaged. Error in the values is limited by the accuracy of the instrument, which is 5% of the raw data values. Sample 3A could not be analyzed due to human error.

4. Photoluminescence emission spectrum

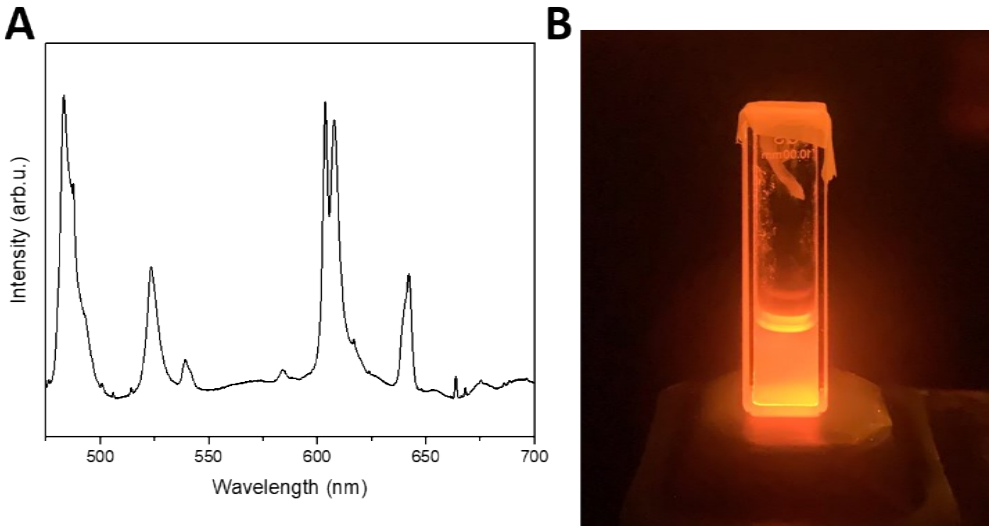

Figure S2 A.) Photoluminescence emission spectrum of sample 4 upon 457.5 nm excitation.B) Camera photo of the luminescence of a dispersion of the nanoparticles in toluene viewed through a 535 nm long pass filter to filter out the excitation light. (pulse energy 33 mJ, pulse width a few ns).

5. Powder X-ray diffraction before and after irradiation

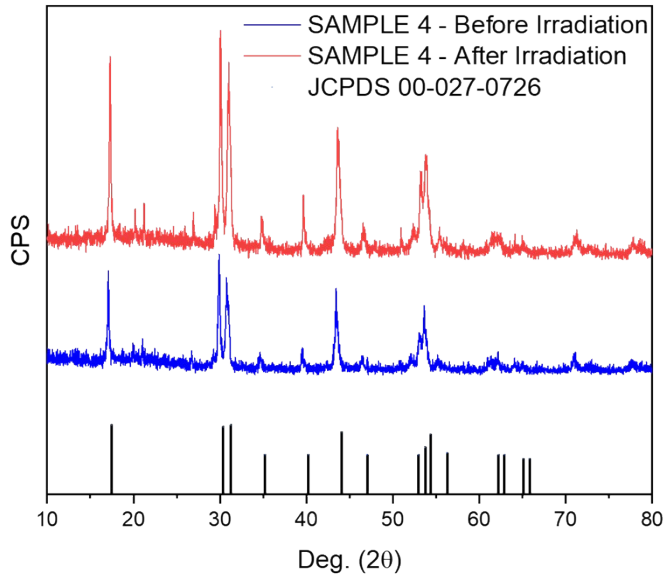

Figure S3. Powder X-ray diffraction of sample 4 before (blue) and after (red) X-ray irradiation (unfiltered, Au anode, 50 kVp, 80 μA).

6. Kinetic profiles of samples 1-4

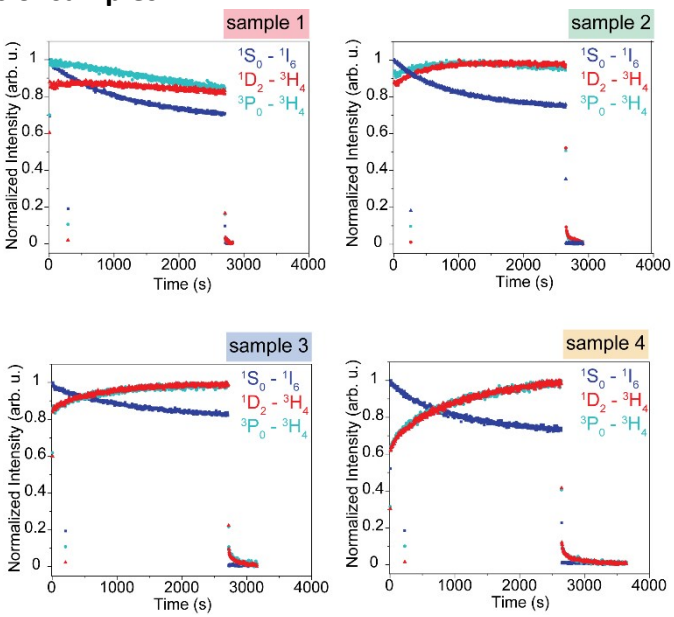

Figure S4. Time-dependent radioluminescence emission kinetics of samples 1-4 plotted as the intensity maximum of the transition vs. time.

7. Band gap extrapolation data

	Ionic radius	Band gap energy					Lowest $4f^{N-1}5d^1$ level	
							Ce^{3+}	Pr^{3+}
Ln		$LnAlO_3$	$LiLnF_4$	$NaLnF_4$			$NaLnF_4$	
		Exp.	Exp.	Exp.	Calc.	Extrapol.	Exp.	Extrapol.
Lu	100	8.3 [2]	11.4[3]	-	8.85[4]	13.8	-	6.55
Y	104	7.9 [5]	11.0 [3]	-	8.50[4]	13.2	5.06[6]	6.57
Gd	108	7.4[7]	10.9[7]	-	7.41[4]	12.7	5.08[6]	6.59
La	117	5.9 [9]	-	11.5	-	11.5	5.15[10]	6.65

Table S2. Experimental, calculated and extrapolated band gap energies of several Ln^{3+} containing crystals (Ln=Y, La, Gd, Lu) and lowest level of the $4f^N$-$5d^1$ configuration of Ce^{3+} (N=1) and Pr^{3+} (N=2), with respect to the electronic ground state, in $NaLnF_4$.

8. Radioluminescence before and after persistent luminescence

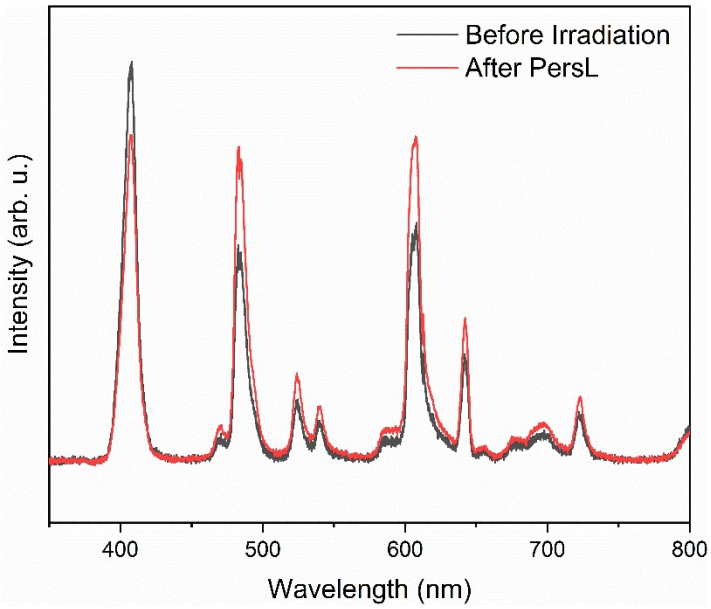

Figure S5. Radioluminescence emission spectrum of sample 4 before irradiation (black) and immediately after persistent luminescence has ceased (red) (Unfiltered X-ray beam, Au target, 50 kVp, 80 µA).

9. Thermoluminescence data after heating cycles

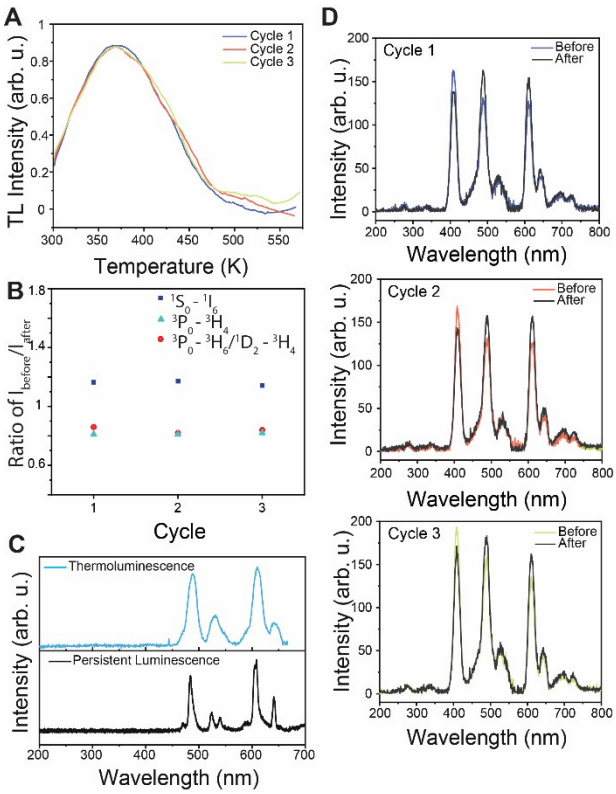

Figure S6. A) Thermoluminescence glow gurves after 3 heating cycles. B) Ratio of emission intensity before/after irradiation of the the $^1S_0 \rightarrow {}^1I_6$, $^3P_0 \rightarrow {}^3H_4$ and $^3P_0 \rightarrow {}^3H_6/{}^1D_2 \rightarrow {}^3H_4$ transitions illustrating the intensity of the transitions can be recovered after each heating cycle. C) Comparison of the thermoluminescence emission spectrum taken at the glow curve maximum (368 K) and the persistent luminescence emission spectrum. D) Thermoluminescence emission spectra before and after each cycle, illustrating the repeatable change and recovery of intensities before and after irradiation and heating.

10. Powder X-ray Diffraction of undoped $NaLuF_4$ nanoparticles

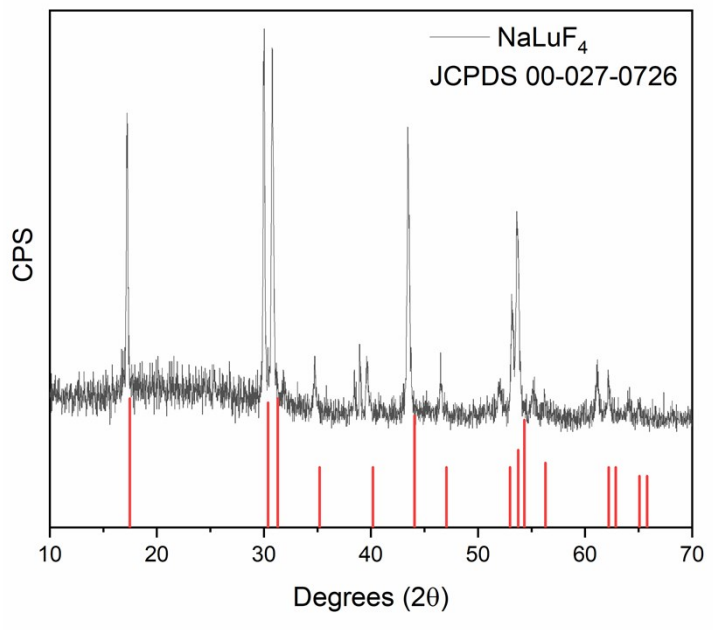

11. TEM of undoped $NaLuF_4$ nanoparticles

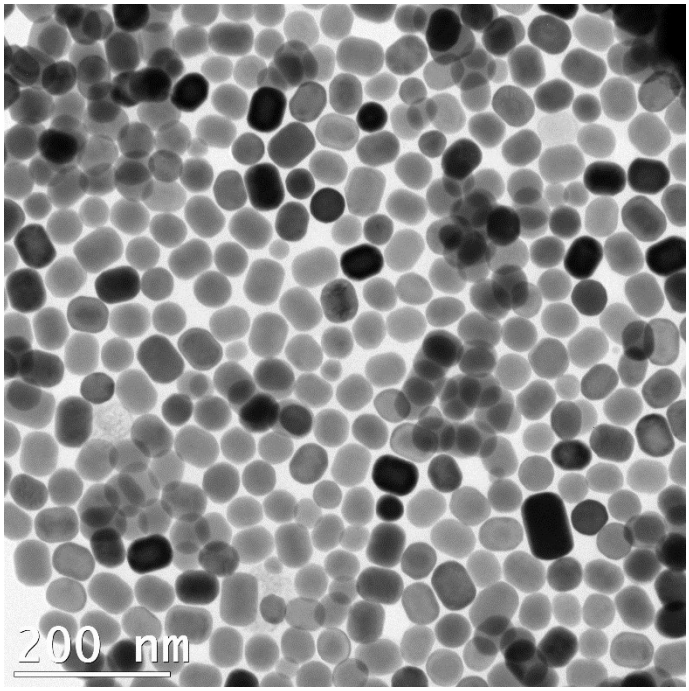

References

1 T. Rinkel, J. Nordmann, A. Raj, M. Haase, *Nanoscale*, 2014, **6**, 14523-14530

2 I. Kamenskikh, C. Pedrini, A. Petrosyan and A. Vasil'ev, *Journal of Luminescence*, 2009, **129**, 1509–1513.

3 N. Yu. Kirikova, M. Kirm, J. C. Krupa, V. N. Makhov, E. Negodin and J. Y. Gesland, *Journal of Luminescence*, 2004, **110**, 135–145.

4 B. Huang, H. Dong, K. L. Wong, L. D. Sun and C. H. Yan, *Journal of Physical Chemistry C*, 2016, 120, 18858–18870.

5 Y. v. Zorenko, A. S. Voloshinovskiĭ and I. v. Konstankevych, *Optics and Spectroscopy (English translation of Optika i Spektroskopiya)*, 2004, **96**, 532–537.

6 P. Dorenbos, *Journal of Luminescence*, 2013, **135**, 93–104.

7 J. W. M. Verweij, M. T. Cohen-Adad, D. Bouttet, H. Lautesse, B. Moine and C. Pédrini, *Chemical Physics Letters*, 1995, **239**, 51–55.

8 M. Kirm, J. C. Krupa, V. N. Makhov, M. True, S. Vielhauer and G. Zimmerer, *Physical Review B - Condensed Matter and Materials Physics*, 2004, **70**, 1–4.

9 S. G. Lim, S. Kriventsov, T. N. Jackson, J. H. Haeni, D. G. Schlom, A. M. Balbashov, R. Uecker, P. Reiche, J. L. Freeouf and G. Lucovsky, *Journal of Applied Physics*, 2002, **91**, 4500–4505.

10 J. Andriessen, E. van der Kolk and P. Dorenbos, *Physical Review B - Condensed Matter and Materials Physics*, 2007, **76**, 075124.